

Polarization-resolved fine-structure splitting of zero-dimensional $\text{In}_x\text{Ga}_{1-x}\text{N}$ excitons

Supaluck Amloy, Y T Chen, K F Karlsson, K H Chen, H C Hsu, C L Hsiao, L C Chen and Per-Olof Holtz

Linköping University Post Print

N.B.: When citing this work, cite the original article.

Original Publication:

Supaluck Amloy, Y T Chen, K F Karlsson, K H Chen, H C Hsu, C L Hsiao, L C Chen and Per-Olof Holtz, Polarization-resolved fine-structure splitting of zero-dimensional $\text{In}_x\text{Ga}_{1-x}\text{N}$ excitons, 2011, PHYSICAL REVIEW B, (83), 20, 201307.

<http://dx.doi.org/10.1103/PhysRevB.83.201307>

Copyright: American Physical Society

<http://www.aps.org/>

Postprint available at: Linköping University Electronic Press

<http://urn.kb.se/resolve?urn=urn:nbn:se:liu:diva-68780>



Polarization-resolved fine-structure splitting of zero-dimensional $\text{In}_x\text{Ga}_{1-x}\text{N}$ excitons

S. Amloy,^{1,2} Y. T. Chen,³ K. F. Karlsson,¹ K. H. Chen,^{3,4} H. C. Hsu,⁴ C. L. Hsiao,⁴ L. C. Chen,⁴ and P. O. Holtz¹

¹*Department of Physics, Chemistry, and Biology, Linköping University, S-58183 Linköping, Sweden*

²*Department of Physics, Faculty of Science, Thaksin University, Phattalung 93110, Thailand*

³*Institute of Atomic and Molecular Sciences, Academia Sinica, Taipei 106, Taiwan*

⁴*Center for Condensed Matter Sciences, National Taiwan University, Taipei 106, Taiwan*

(Received 29 January 2011; published 18 May 2011)

The fine-structure splitting of quantum confined $\text{In}_x\text{Ga}_{1-x}\text{N}$ excitons is investigated using polarization-sensitive photoluminescence spectroscopy. The majority of the studied emission lines exhibits mutually orthogonal fine-structure components split by 100–340 μeV , as measured from the cleaved edge of the sample. The exciton and the biexciton reveal identical magnitudes but reversed sign of the energy splitting.

DOI: [10.1103/PhysRevB.83.201307](https://doi.org/10.1103/PhysRevB.83.201307)

PACS number(s): 78.67.Hc, 73.21.La, 78.55.Cr

Recent quantum information technologies, including quantum cryptography^{1,2} and optical quantum computing,³ are fascinating applications exploiting the quantum properties of single^{4,5} and correlated photons⁶ in order to gain advantage in information processing and data transmission.⁷ Semiconductor quantum dots (QDs) are especially attractive as the light sources for such applications since they can emit the photons on demand.^{4,8} The vast majority of the QDs studied today are based on III-arsenide materials, but the optically efficient III-nitride system provides a wider range of band gaps with extended tunability of the photon color as well as stronger quantum confinement with the potential of room-temperature operation.^{5,6}

A single photon is emitted from the QD when a quantum confined electron-hole pair recombines. In general, the Coulomb interaction between the negatively charged electron (e) and the positively charged hole (h) lifts the fourfold degeneracy of the e - h pair ground level, forming a set of zero-dimensional exciton states of unequal energies. This Coulomb-induced splitting is referred to as the fine-structure splitting (FSS), and the resulting energy level arrangement is strongly dependent on the symmetry of the exciton wave function.

The III-nitride materials crystallize normally as wurtzite, setting the upper limit of the QD symmetry to the point group C_{3v} (Ref. 9), corresponding to a threefold proper rotation axis [0001] (c axis) contained in three vertical reflection planes. The exciton states and the corresponding optically allowed transitions for C_{3v} -symmetry QDs were reported in Ref. 10. For a C_{3v} QD there are two types of excitons: Type 1 consists of two states optically active with polarization vectors in the xy plane perpendicular to the c axis, and type 2 consists of three states, of which one is dark, one is optically active in the xy plane, and the third is active with a vertical polarization vector (see Fig. 1).

The conventional classification of III-nitride bulk excitons is either A , B , or C , depending on which valence band is dominating the hole character. For comparison with bulk excitons, the in-plane polarized A excitons here correspond to type 1, while the B and C excitons have vertical polarization vectors and correspond to type 2.

Any symmetry breaking, lowering the symmetry below C_{3v} , lifts the degeneracy of the x - and y -polarized components (see

Fig. 1). This asymmetry-induced FSS has been thoroughly investigated in other QD systems, e.g., asymmetric zincblende GaAs and InGaAs QDs,^{11,12} and significant effort is focused on minimizing this splitting since it prohibits the emission of polarization-entangled photon pairs in the decay of the biexciton. Note that, in addition to the energy splitting of the x - and y -polarized components with in-plane polarization anisotropy, the asymmetry also gives rise to new vertically polarized components for both types of excitons (see Fig. 1).¹⁰

Recent measurements on the photons emitted from single $\text{In}_x\text{Ga}_{1-x}\text{N}/\text{GaN}$ and $\text{GaN}/\text{Al}(\text{Ga})\text{N}$ QDs reveal strong in-plane polarization anisotropy,¹³ indicating that the actual exciton symmetry is lower than C_{3v} . However, no asymmetry-induced x - and y -polarized FSS has been resolved for the majority of investigations of III-nitride-based QDs until recently,^{13,14} when a huge splitting of 2–7 meV was interpreted as the FSS of exciton states confined in asymmetric GaN/AlN QDs.¹⁵ This splitting is about two orders of magnitude larger than the typical asymmetry-induced FSS for III-arsenide-based systems.

There are several reasons contributing to the difficulty to resolve the FSS for the III-nitride systems: (1) The emission wavelength of the studied structures is typically significantly shorter (2–3 times) than for arsenide systems, reducing the spectral resolution (~ 4 –9 times) for grating based spectroscopy. (2) The emission linewidth (~ 1 meV) is typically a factor 10 wider than for high-quality arsenide systems (20–100 μeV). (3) The integrated degree of polarization for a given QD anisotropy is significantly greater for the III-nitrides as compared to III-arsenides. This effect is related to the ~ 10 –30 times smaller split-off energy for the nitrides and results in one in-plane polarized spectral component with dramatically weaker intensity than the other, making it hard to discern in the spectra.

In order to measure excitonic fine-structure energies for $\text{In}_x\text{Ga}_{1-x}\text{N}$ QDs, it is reasonable to design the experiment with the purpose of resolving the largest FSS, i.e., the splittings present also for symmetric QDs. Such splittings are significantly larger than the asymmetry-induced FSS for weakly asymmetric QDs and are comparable to the asymmetry-induced FSS for strongly asymmetric QDs. Access to the vertically polarized components is also required for these experiments [see Fig. 1(b)].

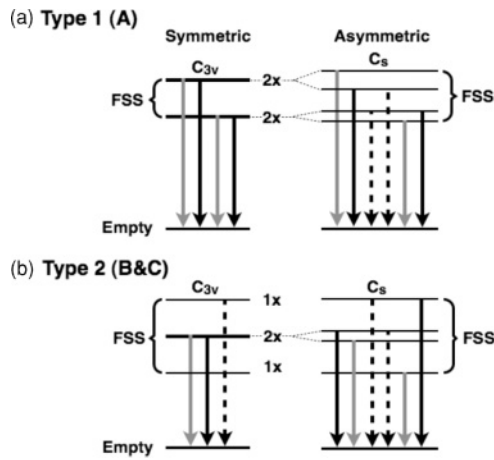


FIG. 1. Schematic decay diagrams for excitons of (a) type 1 and (b) type 2 for symmetric C_{3v} and asymmetric C_s QDs. The gray (black) lines indicate x -polarized (y -polarized) transitions, and dashed lines indicate the z -polarized transitions.

In this work, the FSS of single excitons and biexcitons confined in $\text{In}_x\text{Ga}_{1-x}\text{N}$ potential minima are investigated using two different measurement geometries, accessing either the two in-plane polarization directions or one in-plane as well as the vertical polarization direction, respectively. The FSS is resolved only in the unconventional geometry used to access the vertical polarization vector, and the obtained energy splittings are comparable to the typical values for III-arsenide systems and thus are significantly smaller than the asymmetry-induced FSS recently reported for GaN QDs.¹⁵

The investigated sample was grown on a c -plane sapphire substrate at a temperature of 500°C by plasma-assisted molecular-beam epitaxy.¹⁶ A ~ 2.5 -nm-thick compressively strained $\text{In}_x\text{Ga}_{1-x}\text{N}$ layer (nominally 20% In) was formed on a 230-nm GaN barrier layer and capped with a 30-nm-thick GaN layer.^{17,18} Scanning transmission electron microscopy imaging reveals significant In segregation within the $\text{In}_x\text{Ga}_{1-x}\text{N}$ layer and the formation of QD-like exciton localization centers. The density of optically active localization centers were determined to be in the range 10^9 – 10^{10} cm^{-2} , as estimated from number of sharp emission lines observed in the optical emission spectra.

The microphotoluminescence (μPL) spectra were recorded in a top-view, normal to the c -plane of the sample along the growth direction, as well as in a side-view, normal to the cleaved edge of the sample along the $[10\bar{1}0]$ direction of the crystal. The sample used for the top-view measurements was coated by a 50-nm-thick aluminum layer sparsely perforated by circular openings (diameter of 260 nm). This metal mask reduces the number of localization centers contributing to the recorded spectrum and enables “single-dot spectroscopy.” The sample was mounted on a cold finger inside a cryostat, which was cooled down to 4 K by a continuous flow of liquid helium. A cw laser emitting at 266 nm was focused on the sample with high spatial resolution (~ 2 μm) by a reflecting objective lens. The photoluminescence (PL) signal was collected by the same objective lens and dispersed in a monochromator (focal length of 0.48 m, grating of 1200 grooves/mm) and detected by a liquid-nitrogen-cooled charge-coupled device. The spectral resolution of the system is about 1.3 meV in the

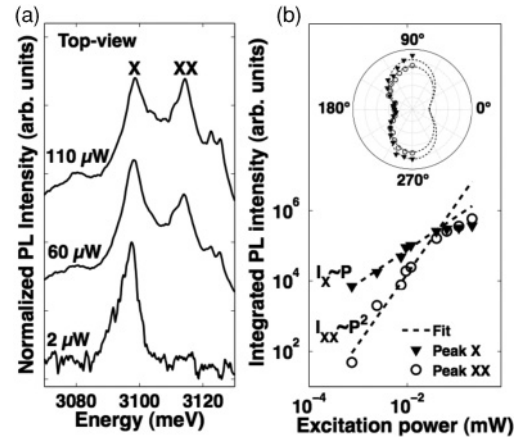


FIG. 2. (a) The μPL spectra of a single $\text{In}_x\text{Ga}_{1-x}\text{N}$ QD-like potential excited with laser powers as indicated, measured for the light emitted in the growth direction. The baselines are successively shifted vertically for clarity. (b) The integrated intensities of X (I_X) and XX (I_{XX}) plotted as a function of excitation powers. The inset shows the polar plots of the linear polarization dependence of peaks X and XX together with fitted lines on the form $\alpha \sin^2 \theta + \beta \cos^2 \theta$, where α and β are constants and θ is the polarization angle.

relevant wavelength range. The polarization of the PL signal was analyzed by a turnable half-wave retardation plate and a fixed linear polarizer in front of the monochromator.

The μPL spectra recorded in top-view, with the excitation power varied from 2 to 110 μW , are shown in Fig. 2(a). In the low-power regime, the integrated intensity of the peaks labeled X and XX develops with linear and quadratic power dependence [see Fig. 2(b)], respectively. Furthermore, both peaks X and XX exhibit identical in-plane polarization angles and polarization degrees, as shown the inset of Fig. 2(b). The polarization dependence of the interband recombination is determined solely by the holes, which yields identical polarization for all emission lines originating from the same confinement potential with the recombining hole in the ground state. It can therefore be concluded that the two peaks X and XX most likely originate from the same QD-like potential. The linear and quadratic power dependencies of peaks X and XX justify their attribution to the exciton and the biexciton,¹⁹ respectively, with the corresponding biexciton negative binding energy of -16 meV. Negative binding energies have been reported previously for biexcitons in $\text{In}_x\text{Ga}_{1-x}\text{N}$ QDs.^{20,21} From the x - and y -polarized spectra of peaks X and XX, no FSS could be resolved for this or other QDs measured in this geometry.

A typical spectrum of the cleaved-edge emission is presented in Fig. 3, extracted along the $[10\bar{1}0]$ direction and obtained with excitation powers ranging from 80 to 470 μW . Only a few sharp emission peaks are observable, indicating that only a small number of QD-like potential minima are within the focus and penetration depth of the laser. Similar to the top-view measurements, the intensity of some emission lines (labeled 1, 2, and X) saturates when the power is increased, while the intensity of other peaks (labeled 3 and XX) takes over at high power, indicating the formation of multiexciton complexes at high excitation powers.

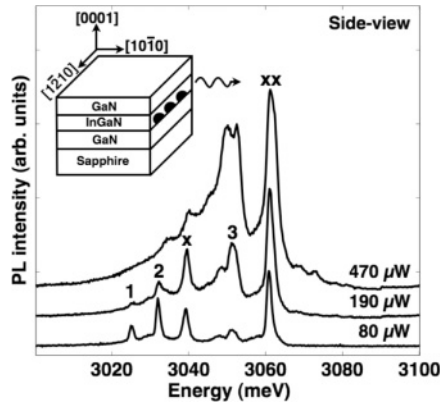


FIG. 3. The μ PL spectra of $\text{In}_x\text{Ga}_{1-x}\text{N}$ QD-like potentials excited with laser powers as indicated, measured for the light emitted in the $[10\bar{1}0]$ direction. The baselines are successively shifted vertically for clarity. The inset shows a schematic and orientation of the sample.

Polarization-resolved spectra are shown in Fig. 4 for linear polarization vectors parallel to the $[1\bar{2}10]$ direction (solid line) and parallel to the growth direction $[0001]$ (dashed line). The two peaks labeled X and XX originate from the same QD-like potential since both peaks are strongly polarized along the c axis with the same degree of polarization, $\sim 65\%$. Peaks 1–3 are also polarized along the c axis, but to different degrees (1, 19%; 2, 35%; and 3, 84%). Thus, peaks X and XX are interpreted as the exciton and the biexciton (binding energy of -22 meV) of the same confinement potential, respectively.

The biexciton XX is a singlet state, and the various components of the emission spectrum of XX are produced solely by the set of final states X, which, in general, are energetically split due to FSS, as shown in the right inset of Fig. 5 for two dominating optical transitions. Thus, the spectral pattern of XX is simply the mirrored pattern of X.

An expanded view of the normalized polarization-resolved spectra of peaks X and XX is shown in Fig. 5. Two linearly polarized components are visible for peaks X and XX. The magnitude of the energy splitting, 250 μeV , is identical for

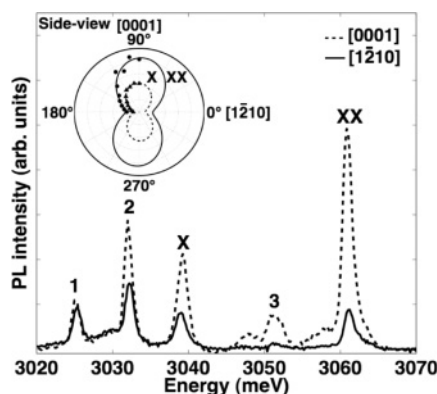


FIG. 4. Polarization-resolved μ PL spectra of the $\text{In}_x\text{Ga}_{1-x}\text{N}$ QD-like potentials recorded for linear polarization vectors along $[0001]$ and $[1\bar{2}10]$. The inset shows polar plots of the linear polarized emission of peaks X and XX together with the fitted lines, as in Fig. 2(b).

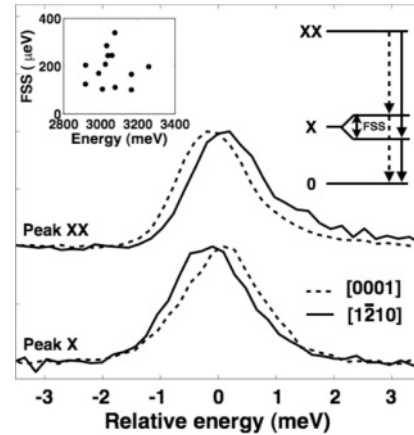


FIG. 5. The expanded view of the polarization-resolved spectra of peaks X and XX. All spectra are normalized, and the baseline of peak XX is shifted vertically for clarity. The insets show the fine-structure splitting of 14 emission lines plotted as a function of their energies (left) and the schematic of the cascade decay of XX and X (right).

both. However, the signs of the splitting are reversed for peaks X and XX, as expected for the exciton and biexciton. This result confirms the interpretation that peaks X and XX belong to the same QD-like potential and that the polarization-resolved components are, indeed, due to the FSS. The other emission lines in Fig. 4 exhibit different values of the splitting (1, 210 μeV ; 2, 290 μeV ; and 3, unresolved).

Several other emission lines were investigated from the cleaved edge, and a similar FSS was systematically resolved for the majority of them, with magnitudes ranging between ~ 100 and ~ 340 μeV , as summarized in the left inset of Fig. 5. The emission lines, which did not reveal any FSS, can originate from charged exciton complexes for which zero splitting is expected.^{13,22} The large variation of the FSS energy is attributed to the inherent randomness in size, shape, and depth of the studied confinement potentials, and no clear correlation between FSS and the emission energy can be found (see the left inset in Fig. 5).

Some of the studied emission lines have significant vertically polarized components (see Fig. 4), suggesting that the corresponding excitons originate from type 2, related to the bulk excitons of types B or C, with dipole-allowed transitions for vertical polarization vectors [see Fig. 1(b)]. The FSS has been estimated to be very small for free B excitons in unstrained bulk GaN ($\Gamma_1 - \Gamma_5 \leq 10$ μeV),^{23,24} but it becomes enhanced in the presence of a biaxial strain, and an experimentally determined splitting of ~ 250 μeV has been reported.²³ For GaN bulk C excitons, the FSS is ~ 500 μeV without strain.²³

The B and C excitons correspond to excited states for bulk materials, but the type 2 excitons can become the ground state in QDs and other exciton localization centers by either tensile biaxial strain or by a small aspect ratio of the confinement potential, with the lateral localization length smaller than the vertical. The $\text{In}_x\text{Ga}_{1-x}\text{N}/\text{GaN}$ structures investigated in this work are compressively strained, suggesting that a strong lateral confinement is the reason for localization centers emitting predominantly z -polarized light and, accordingly, the

reason for the reversing of the valence band order. Inversion of the hole ground state has been systematically investigated for well-controlled zincblende systems, and a transition from heavy- to light-hole types has been concluded to occur when the lateral and vertical localization lengths become comparable, both for unstrained AlGaAs structures²⁵ and for compressively strained InAs/GaAs structures.²⁶ The same holds qualitatively for wurtzite, with the modification that the crystal field splitting and the strong vertical piezoelectric field (effectively reducing the vertical localization length) may shift the critical QD aspect ratio for inversion to values smaller than unity. The dominating lateral confinement for the $\text{In}_x\text{Ga}_{1-x}\text{N}/\text{GaN}$ structures found to be responsible for the reversion of valence band implies that the lateral fragmentation of the In composition in the $\text{In}_x\text{Ga}_{1-x}\text{N}$ layer occurs on a length scale below the layer thickness, ~ 2.5 nm. This is consistent with scanning transmission electron microscopy (STEM) studies of the In composition in the $\text{In}_x\text{Ga}_{1-x}\text{N}$ layer, which reveal clusters of increased In composition with lateral sizes, mainly in the range 1–5 nm. Note that, although most of the emission lines shown in Fig. 4 exhibit predominant z polarization, this is only the case for $\sim 50\%$ of all the studied emission lines studied from the cleaved edge.

The measured FSS is interpreted as the combined effect of the inherent splitting of a symmetric exciton with additional asymmetry-induced splitting [see Fig. 1(b)]. It should be noted that the FSS values < 350 μeV obtained in this work for

confined $\text{In}_x\text{Ga}_{1-x}\text{N}$ excitons are comparable with the values of strained bulk GaN.^{23,24} This may appear surprising since quantum confinement is known to enhance the Coulomb interaction, yielding significantly larger values of the FSS for QDs as compared to bulk.²⁷ On the other hand, the strong built-in piezoelectric field in strained $\text{In}_x\text{Ga}_{1-x}\text{N}$ QDs^{13,17} effectively separates the electrons and holes spatially and thereby weakens the e - h Coulomb interaction. Thus, the resulting magnitude of the FSS is determined by the competition between the quantum confinement and built-in electric fields of the heterostructure.

In summary, the narrow μPL spectra of the exciton and biexciton of $\text{In}_x\text{Ga}_{1-x}\text{N}$ QD-like potentials were identified by power-dependence measurements combined with the polarization-resolved FSS analysis as measured from the cleaved edge of a sample. The magnitudes of the FSS were found to be in the range 100–340 μeV , i.e., values comparable to bulk GaN excitons. The large variation of FSS was uncorrelated with the emission energy and reflects the randomness of size and indium composition for the potential minima.

This work has been supported by a Ph.D. scholarship from Thaksin University in Thailand for S. Amloy, grants from the Swedish Research Council (VR), the Nano-N consortium funded by the Swedish Foundation for Strategic Research (SSF), and the Knut and Alice Wallenberg Foundation. The authors are thankful for XRD and STEM measurement by J. Palisaitis and for fruitful discussions with P. P. Paskov.

-
- ¹C. Kurtsiefer, P. Zarda, M. Halder, H. Weinfurter, P. M. Gorman, P. R. Tapster, and J. G. Rarity, *Nature (London)* **419**, 450 (2002).
²C. Z. Peng *et al.*, *Phys. Rev. Lett.* **94**, 150501 (2005).
³D. Loss and D. P. DiVincenzo, *Phys. Rev. A* **57**, 120 (1998).
⁴P. Michler *et al.*, *Science* **290**, 2282 (2000).
⁵S. Kako, C. Santori, K. Hoshino, S. Götzinger, Y. Yamamoto, and Y. Arakawa, *Nat. Mater.* **5**, 887 (2006).
⁶P. Michler, A. Imamoğlu, M. D. Mason, P. J. Carson, G. F. Strouse, and S. K. Buratto, *Nature (London)* **406**, 968 (2000).
⁷C. Monroe, *Nature (London)* **416**, 238 (2002).
⁸C. Santori, M. Pelton, G. Solomon, Y. Dale, and Y. Yamamoto, *Phys. Rev. Lett.* **86**, 1502 (2001).
⁹P. Tronc, K. S. Zhuravlev, V. G. Mansurov, G. F. Karavaev, S. N. Grinyaev, I. Milosevic, and M. Damnjanovic, *Phys. Rev. B* **77**, 165328 (2008).
¹⁰K. F. Karlsson, M. A. Dupertuis, D. Y. Oberli, E. Pelucchi, A. Rudra, P. O. Holtz, and E. Kapon, *Phys. Rev. B* **81**, 161307R (2010).
¹¹D. Gammon, E. S. Snow, B. V. Shanabrook, D. S. Katzer, and D. Park, *Phys. Rev. Lett.* **76**, 3005 (1996).
¹²S. Seidl *et al.*, *Phys. E* **40**, 2153 (2008).
¹³R. Bardoux *et al.*, *Phys. Rev. B* **77**, 235315 (2008).
¹⁴R. Bardoux, A. Kaneta, M. Funato, Y. Kawakami, A. Kikuchi, and K. Kishino, *Phys. Rev. B* **79**, 155307 (2009).
¹⁵C. Kindel *et al.*, *Phys. Rev. B* **81**, 241309R (2010).
¹⁶C. L. Hsiao *et al.*, *Appl. Phys. Lett.* **92**, 111914 (2008).
¹⁷D. Simeonov, A. Dussaigne, R. Butté, and N. Grandjean, *Phys. Rev. B* **77**, 075306 (2008).
¹⁸M. Kryško *et al.*, *Appl. Phys. Lett.* **91**, 211904 (2007).
¹⁹K. Brunner, G. Abstreiter, G. Böhm, G. Tränkle, and G. Weimann, *Phys. Rev. Lett.* **73**, 1138 (1994).
²⁰K. Sebald, H. Lohmeyer, J. Gutowski, T. Yamaguchi, and D. Hommel, *Phys. Status Solidi B* **243**, 1661 (2006).
²¹R. Seguin *et al.*, *Appl. Phys. Lett.* **84**, 4023 (2004).
²²J. J. Finley, D. J. Mowbray, M. S. Skolnick, A. D. Ashmore, C. Baker, A. F. G. Monte, and M. Hopkinson, *Phys. Rev. B* **66**, 153316 (2002).
²³P. P. Paskov, T. Paskova, P. O. Holtz, and B. Monemar, *Phys. Rev. B* **64**, 115201 (2001).
²⁴B. Monemar, P. P. Paskov, J. P. Bergman, A. A. Toropov, T. V. Shubina, T. Malinauskas, and A. Usui, *Phys. Status Solidi B* **245**, 1723 (2008).
²⁵Q. Zhu, K. F. Karlsson, E. Pelucchi, and E. Kapon, *Nano Lett.* **7**, 2227 (2007).
²⁶T. Kita, O. Wada, H. Ebe, Y. Nakata, and M. Sugawara *Jpn. J. Appl. Phys.* **41**, L1143 (2002).
²⁷T. Takagahara, *Phys. Rev. B* **47**, 4569 (1993).